atmosphere

MDPI

Article

Study on Thermal Storage Wall Heating System of Traditional Houses in Cold Climate Zone of China: A Case Study in Southern Shaanxi

Shuo Chen [1,*], Simin Yang [2,*], Wensheng Mo [1], Bart J. Dewancker [1], Jing Mao [3] and Jie Chen [3]

[1] Faculty of Environmental Engineering, The University of Kitakyushu, Kitakyushu 808-0135, Japan
[2] School of Design, Xianyang Normal University, Xianyang 712000, China
[3] School of Electronic and Information Engineering, Ankang University, Ankang 725000, China
* Correspondence: b0dbb010@eng.kitakyu-u.ac.jp (S.C.); a9dbb415@eng.kitakyu-u.ac.jp (S.Y.); Tel.: +86-18729288718 (S.C.); +86-13891029853 (S.Y.)

Abstract: Solar energy has the advantages of being green, renewable, and energy-efficient. The use of solar energy in buildings can result in significant energy savings, and a great deal of practical and theoretical research has been conducted on solar buildings around the world. Southern Shaanxi belongs to a climate zone with hot summers and cold winters (HSCW). The mean room temperature is 4 °C, and it is lower than 2 °C at night, which greatly exceeds the thermal comfort range that the human body can bear. Aiming at a range of challenges including backward heating methods and low heating efficiency in southern Shaanxi, a fully passive thermal storage wall heating system (TSWHS) is proposed for traditional houses in the area. The specific method is to set up a thermal storage wall (TSW) outside the outer walls on the east, west, and south sides of the residential buildings. The wall is provided with an air exchange port, and there is no glass in the outer area of the doors and windows, which does not affect the normal application. The principle is that after the TSW receives solar radiation, the temperature of the internal HDPE (high-density polyethylene) and the air inside the cavity rises, which raises the interior temperature via the heat transfer and the air exchange port inside the TSW. The hot air inside the thermal wall achieves the purpose of heating. Lastly, through a comparison with the original heating system (OHS), it is confirmed that the TSWHS has certain practicability. According to an experimental simulation, the system can increase the indoor temperature by an average of 5.1 °C in winter and save about 1726.43 kWh of energy, accounting for 27.24% of the energy saving.

Keywords: cold climate zone; traditional houses; thermal storage wall heating system (TSWHS); HDPE; energy saving

check for updates

Citation: Chen, S.; Yang, S.; Mo, W.; Dewancker, B.J.; Mao, J.; Chen, J. Study on Thermal Storage Wall Heating System of Traditional Houses in Cold Climate Zone of China: A Case Study in Southern Shaanxi. *Atmosphere* **2022**, *13*, 2049. https://doi.org/10.3390/atmos13122049

Academic Editor: Marco Ferrero

Received: 4 November 2022
Accepted: 4 December 2022
Published: 7 December 2022

Publisher's Note: MDPI stays neutral with regard to jurisdictional claims in published maps and institutional affiliations.

Copyright: © 2022 by the authors. Licensee MDPI, Basel, Switzerland. This article is an open access article distributed under the terms and conditions of the Creative Commons Attribution (CC BY) license (https://creativecommons.org/licenses/by/4.0/).

1. Introduction

1.1. Motivation

From 2010 to 2019, global residential energy consumption gradually increased, and the share of energy demand for residential housing in China increased from 14.85% to 16.31% of total energy consumption [1]. Therefore, residential buildings have become one of the industries with high energy consumption in China. To address this problem, many scholars have proposed related technologies for energy saving, such as the use of wind energy, nuclear energy, solar energy, etc. to replace fossil fuels [2]. In China, for energy-saving research, the government has issued many energy-saving design guidelines and made great progress [3]. However, this is rare in rural areas, mainly due to the complex climatic zoning in China and the diversity of residential forms [4]. The majority of traditional houses were constructed by the residents on their own and are characterized by the traditional local culture [5], leading to excessive energy depletion and high carbon exhaustion [6]. In terms of space, they are relatively more spacious than urban residential buildings and have

courtyard space [7]. This spatial feature facilitates the renovation of residential buildings [8]. Under the policy of revitalizing China's rural areas, rural areas have been well developed and rural buildings are increasing year by year, which also directly leads to an increase in energy depletion and carbon exhaustion of rural buildings [9]. Research on building energy efficiency in villages is imminent [10]. Therefore, TSWHS was proposed to solve this problem by combining the characteristics of cold and wet winters in southern Shaanxi.

1.2. Previous Research

Scholars around the world have conducted many theoretical studies and practical explorations on winter building energy efficiency, such as the effects of passive heating design [11], building energy efficiency [12], and solar buildings [13] and their optimization [14].

Most of the research about passive heating design focuses on the fundamentals of the design of heating and the utilization of other energy sources for heating. Underground water storage tanks [15], fresh air systems with windows [16], and solar thermal air heating systems [17] are used for heating in buildings. For areas with poor solar radiation, air source heat pumps can be used for heating [18]. Elmetwalli [19] and Liu [20] modified solar water heaters and combined them with other heating methods, and both heating efficiencies were improved. Chi et al. proposed a passive dual heat and dual cooling system and applied it to a new building and obtained a 39% energy saving through numerical simulations [21]. Wang [22], Aksoy [23], and Brown [24] optimized passive heating in terms of building design, as well as building parameters, which also led to the improved thermal insulation of the building. Givoni conducted a comprehensive theoretical study of solar heating systems, which provided some guidance for future research [25]. Wang proposed a passive design strategy in China, which plays a part in promoting solar energy in China [26]. These studies have improved indoor thermal comfort to some extent, but only in a theoretical way or only by adding other energy sources for heating, and other factors that affect indoor temperature were not discussed.

Most research on building energy efficiency concentrated on changing energy-intensive traditional energy sources and improving the thermal insulation of the envelope. Kuşkaya [27], Wang [28], Gao [29], and He [30] proposed combining residential buildings with solar energy to greatly decrease building energy depletion. Feng simulated and optimized the program configuration of residential houses in the village to reduce energy consumption significantly [31]. Ménard [32] designed windows retrofitted with adjustable elements, and the results confirmed the high energy-saving potential of this method. Liu used solar energy combined with a coal stove for heating, which resulted in a significant reduction in energy consumption [33]. Dabaieh [34], Zhang [35], Mi [36], and Kalbas [37] achieved energy savings by improving the envelope Tadeu [38] and Wang [39] proposed energy-saving practices in terms of theoretical analysis. These studies give guidance and practices for research on aspects of building energy efficiency, but only in terms of changing energy sources or changing the insulation performance of the envelope, with limited energy savings.

For the study of solar buildings, Wang [40] and Bakos [41] proposed algorithms and control of solar energy as a heating system from the theoretical aspect. Sun proposed the incorporation of phase change materials (PCMs) in TSW and concluded that it is effective for increasing the room temperature by studying the heat transfer process [42]. Chandel [43], Athianitis [44], Badescu [45], and Arkar [46] confirmed using solar heating can reduce energy consumption by simulating a solar building. Stevanovic studied optimization strategies for passive solar design and concluded that a combination of various strategies can improve energy efficiency [47]. Li et al. converted a new house in Sichuan into a solar building. The simulated indoor temperature ranged from 8.5 to 21.2 °C, which greatly improved the heat and comfort in the region in winter [48]. Zhou proposed a new enclosure with a multi-slab solar energy accumulation wall with a 20% increase in heating effectiveness [49]. Guo studied a solar heating system, developed a mathematical model, and proposed three evaluation indices. A temperature increase of 55.2% was obtained [50]. These studies investigate solar buildings in terms of theory, simulation,

or practice, improving the theory in this subject area, but the factor of the presence and absence of solar radiation should be considered in the simulation process, which is also an important factor in comparing and verifying the TSWHS for indoor temperature increase.

To sum up, academics have conducted many theoretical studies and retrofitting practices on winter building heating, and they have achieved fruitful results. However, overall, it includes adding passive heating to existing buildings, using solar energy as an adjunct to other heating methods, and separate studies on the impact of changing the insulation properties of the enclosure on building heating. Single studies are always limited in their effect on the indoor temperature, as well as skills. This study proposes the use of solar heating while changing the insulation properties of the envelope (adding HDPE, as well as a glass interlayer), while considering the factors of the influence of the presence or absence of solar radiation on room temperature, for winter heating of conventional houses, to fill the gap in this field.

1.3. Scientific Innovation

It is cold and wet in the winter in southern Shaanxi. According to the survey, the average room temperature is around 3 °C or even below 0 °C, which is seriously beyond the low temperature level that the human body can bear. The existing heating methods such as charcoal fire and electrical appliances have a low heating efficiency and poor heating effect, which can only raise the local interior temperature, and they also have the disadvantages of high carbon emission and high energy consumption. To enhance the indoor temperature and save energy, a TSWHS is proposed (HDPE, hot air exchange thermal storage dual system), which can significantly enhance the internal temperature, extend the heating time and reduce energy consumption.

1.4. Research Purpose

On the basis of the principles of solar radiation, the current residence is modified, and the TSWHS is designed to increase the indoor temperature. ANSYS and EnergyPlus software is used to verify the performance of the system. The following aspects are addressed in this study:

1. The thermal efficiency of TSWHS;
2. The applicable time of the TSWHS throughout the year;
3. The TSWHS reduction in heat load and energy savings throughout the year.

2. Methodology

2.1. Current Situation Research

2.1.1. Research Scope

The case study considered southern Shaanxi, part of Shaanxi Province, China (Figure 1a,b), one of the three natural regions in Shaanxi Province, located in the Qinba Mountain Range, with a total area of 69,929 km^2, including the city of Shangluo, Ankang, and Hanzhong. It is located in the middle of the Qinba Mountain Range, and the Han River runs through the middle. Its geographical pattern of "two mountains interspersed with one river", humid north subtropical continental monsoon climate, vertical zonal geographical diversity, and rich water resources have distinctive regional characteristics. The combination and linkage of the natural geomorphological type in the regional climatic and resource conditions determine the spatial combination and association of the living environment in southern Shaanxi, and the cultural consciousness of the traditional living activities following the natural pattern has formed differences in the village distribution. The majority of traditional villas in the region are arranged in cluster form, and most of the residential construction features 1–2 stories. The most numerous layout forms are line type, L type, and U type.



(**a**) (**b**)

Figure 1. (**a**) Map of China—location of Shaanxi; (**b**) map of Shaanxi—location of Southern Shaanxi.

2.1.2. Climate Characteristics

China's construction climate is divided into seven divisions, and Southern Shaanxi is the region of HSCW (Figure 2a). Shaanxi Province is divided int o three climatic regions from the south to the north: the northern subtropical region, the warm temperate region, and the mid-temperate region, with each climatic zone divided into humid, semi-humid, semi-arid, and arid types of climates (Figure 2b). The annual average wind speed in Southern Shaanxi is low, 2 m/s to 3 m/s in most areas, with a minimum of 0.8 m/s. The ground wind is influenced by the complex terrain; the wind direction is erratic and occurs in all wind directions all year round (Figure 2c). The weather in Southern Shaanxi belongs to the subtropical north and the warm temperate south and is categorized into different types depending on the region. The climates in Southern Shaanxi are diverse, with an ordinary temperature of 13 to 15 °C, an artificial temperature of −1 to 2 °C in January, and an average temperature o f 25 to 27 °C in July (Figure 2d). The total yearly average solar radiation in Southern Shaanxi gradually increases from south to north due to the influence of cloudiness and sunshine hours in different regions, with the lowest level of 3.69 × 109 J/m^2 in the south and the highest level of 5.02 × 109 J/m^2 in the north. Under the influence of sunshine conditions, the sites of mountain settlements in Southern Shaanxi are mostly located on the sunny slope.

2.1.3. Research Methodology

Several research methods were used. First, a field survey of the dwellings in southern Shaanxi was conducted. Measurements, photographs, questionnaires, and interviews were used to understand the style, scale, materials, and physical environment of the dwellings, and to record information about the dwellings, mainly including building forms, structures, dimensions, materials, information on doors and windows, indoor and outdoor temperature, and heating methods. Second, a literature review was performed through combing, reading, analyzing, and summarizing many relevant books, journals, and theoretical materials, to comprehensively understand the domestic and foreign research status related to passive heating and then to obtain its research progress in academia. Lastly, a summarization was conducted to inductively analyze the basic data, select typical dwellings as the research object, and study the thermal storage performance, thermal insulation efficiency, and economic cost of different wall materials, to provide strong support for the selection of thermal storage materials for passive heating systems.

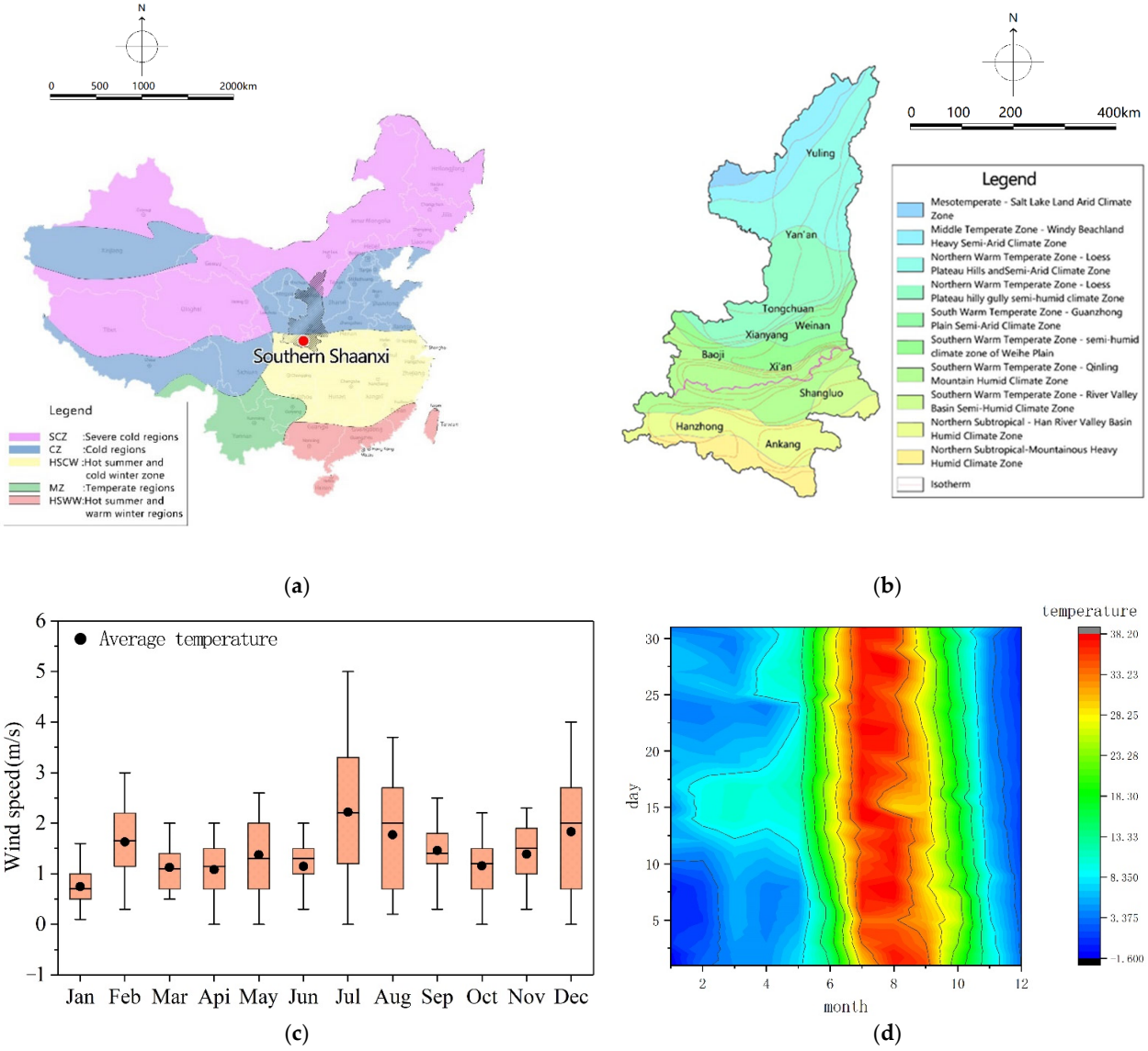


Figure 2. (**a**) Building climate zoning map of China; (**b**) Shaanxi climate zone map; (**c**) wind speed; (**d**) annual temperature variation.

2.1.4. Evaluation Indices

According to the Chinese building industry's energy conservation design standard, the indoor heat ambient design index for heating in winter is that the interior design temperature of the bedroom and living room should be taken as 18 °C [51]; hence, this study used 18 °C to evaluate the improvement effect of internal thermal comfort of the TSWHS as the threshold value of indoor thermal comfort temperature. Furthermore, the PMV-PPD thermal comfort evaluation indices were used to assess the residents' perception of indoor thermal comfort. The principle was proposed by the Danish scholar Fanger in the 1970s. The indices are based on his famous thermal comfort balance equation, which considers six parameters: two human factors, namely, activity level and clothing, and four thermal environmental factors [52].

The thermal comfort equilibrium equation is established on the basis of the basic thermal equilibrium equation, where Qe is replaced by the body regulation function in the peaceful state, Qe* in the comfortable state, according to the skin surface temperature Ts in the peaceful state. Calculating Qr and Qe in the basic heat balance equation, the radiation heat transfer and convection heat transfer obtained are denoted as Qr* and Qe*, respectively.

According to some combinations of these six parameters, the equations are as follows:

$$\mathrm{Qm} - Qe^* \pm Qr^* \pm Qc^* = \Delta Q^*. \quad (1)$$

If ΔQ* = 0, the thermal environment is considered to be comfortable.

If ΔQ* = L ≠ 0, the thermal comfort balance is destroyed. To maintain normal body temperature, the working intensity of the regulating function is bound to change. A higher value of L in absolute terms indicates a larger degree of discomfort. According to the experiment, Fanger obtained a functional relationship of the PMV index representing thermal sensation, thermal load L, and other factors:

PMV is the thermal sensation value of a combination of environmental factors during the experiment. The relationship between this index and human thermal sensation is shown in Table 1.

Table 1. PMV-PPD evaluation indices.

Hot Sensation	Cold	Cool	Slightly Cooler	Neutralize	Slightly Warmer	Warm	Hot
PMV	−3	−2	−1	0	1	2	3

2.1.5. Research Content

According to the research, local people mainly use two types of heating. Active heating mainly uses household appliances, while passive heating mainly uses firewood. These two methods can only increase the local temperature indoors, not the overall temperature. According to the study, the key to the design of this system was the addition of HDPE and the optimization of the wall insulation performance. By comparing the thermal properties of several commonly used thermal insulation materials, HDPE's comprehensive performance is better. After multiple considerations, the outer wall was transformed into a TSW. The temperature rises and the house is heated, while air exchange vents inside the TSW are used to exchange the hot air inside the TSW and the room. Thus, the internal temperature is enhanced by the combined effect of the two systems. Internal temperature variations were analyzed for TSWHS and OHS systems with and without solar radiation, respectively. The optimal heating system is also derived by comparing the heating effect of the four cases. Lastly, heating efficiency, heating time, energy saving, and thermal comfort were studied. The research framework is illustrated in Figure 3.

2.2. Induction of TSWHS

2.2.1. System Design

The study revealed that most of the traditional dwellings in southern Shaanxi are "line" or "L" type, and most of the space occurs in three rooms. The roof form is a pitched roof, and the material is mostly tile or slate. The walls are brick, and the outer layer is lime plaster. On the basis of the architectural information of the current residential house, we used Rhino software to build a residential model with a sloped roof form, with dimensions of 5.1 m × 17.7 m and a total height of 8.2 m, of which the first-floor height was 3.6 m, and the second-floor height was 2.8 m. The height of the sloped roof is 1.8 m (Figure 4a). The Southern Shaanxi area has good sunshine conditions, and the building structure is simple; hence, it is more suitable to set up a TSWHS (Figure 4b). Since most of the houses in southern Shaanxi are oriented north–south, the design of the TSWHS is mainly to transform the walls on the south, east, and west sides. A glass layer was added on the outside of the three walls on the west, south, and east sides with a distance of 100 mm between the glass and wall. There is a layer of air inside, PCMs are added on the outside of the walls as a thermal storage layer, and ventilation holes are made in the walls at a certain distance. The heating storage material of the wall is HDPE, and the thickness is 10 mm. The glass is a single layer of ordinary glass with a light transmittance of 0.87 and a thickness of 6 mm. The wall material information is shown in Figure 5.

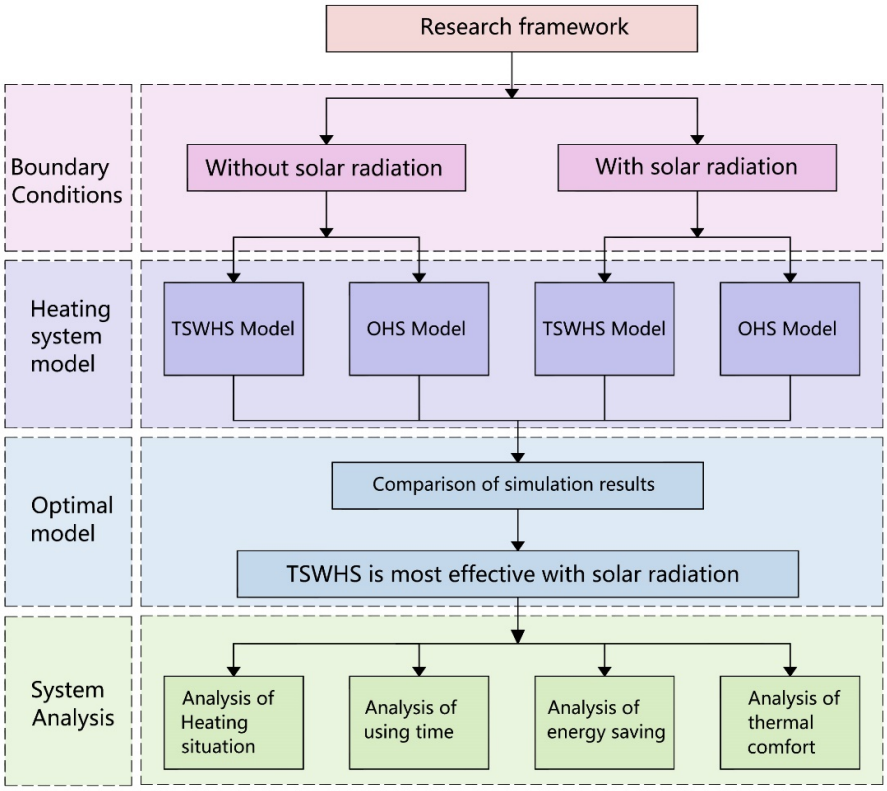


Figure 3. Research framework.

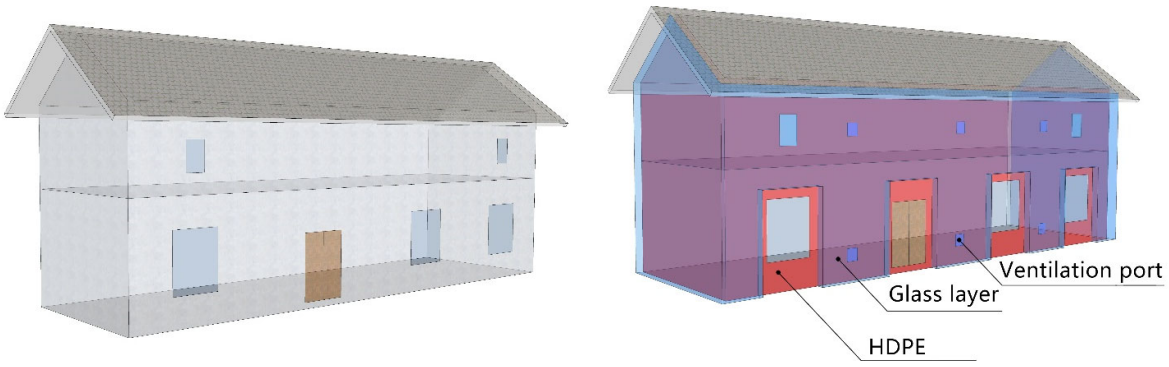


Figure 4. (**a**) Residence model; (**b**) introduction to the main parts of TSWHS.

Li et al. investigated PCM by melt mixing and aqueous solvent etching combined with simple vacuum impregnation, which finally solved the shortcomings of leakage and geothermal conduction present in PCM. The results showed that the upgraded HDPE material had 2.94 times higher thermal conductivity than before, with an enthalpy of melting of 153.95 J/g and an enthalpy of crystallization of 152.82 J/g, which is valuable for electrical and thermal energy storage [53]. The density of HDPE is 964 kg/m^3 [54], the thermal conductivity is 0.36 W/m·K, and the specific thermal capacity is 2301 J/Kg·K [55]; compared with bricks and other materials, its thermal conductivity is low, and it has high thermal storage performance [56]. The heat can be fully absorbed during the day and becomes exothermic at night such that the heat flows to the glass interlayer as well as the interior, which can extend the time of heating the interior. Therefore, HDPE was chosen as the PCMs for TSW. During the day, the air inside the wall was heated, and the outside glass was HDPE, which heated the TSW and warms the room. Meanwhile, the heated air inside the glass cavity was exchanged via vents with the cold air in the room. In the case of

the dual-system heating, the room temperature was increased. The working principle is that HDPE absorbs and stores heat from solar radiation and utilizes the properties of the thermal storage material to raise the room temperature at night.

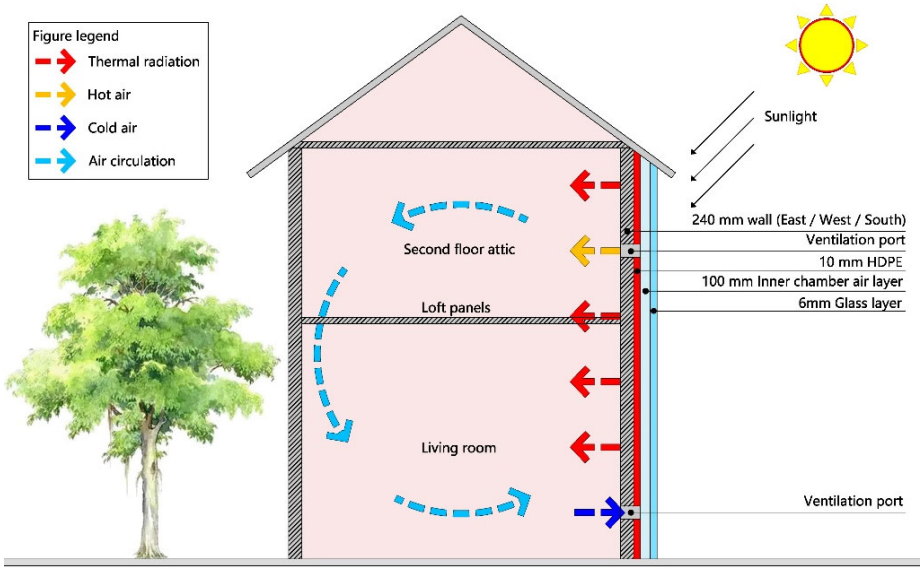


Figure 5. Induction of the TSWHS.

2.2.2. Operating Principle

The principle of TSWHS is using solar radiation to heat the HDPE and air layer (Figure 5). The hot air is exchanged with the cold air in the room through the vents, and the interior temperature is increased with dual system heating. Therefore, TSWHS can be considered a solar heating and recovery device. Multiple factors influence the entire heat transfer process in TSWHS, such as solar radiation, thermal properties of the thermal storage material, thickness, glazing size, room dimensions, and the internal and external temperature of the inflatable layer. To clearly illustrate the heat transfer principle of this system, it is presented in three processes (Figure 6).

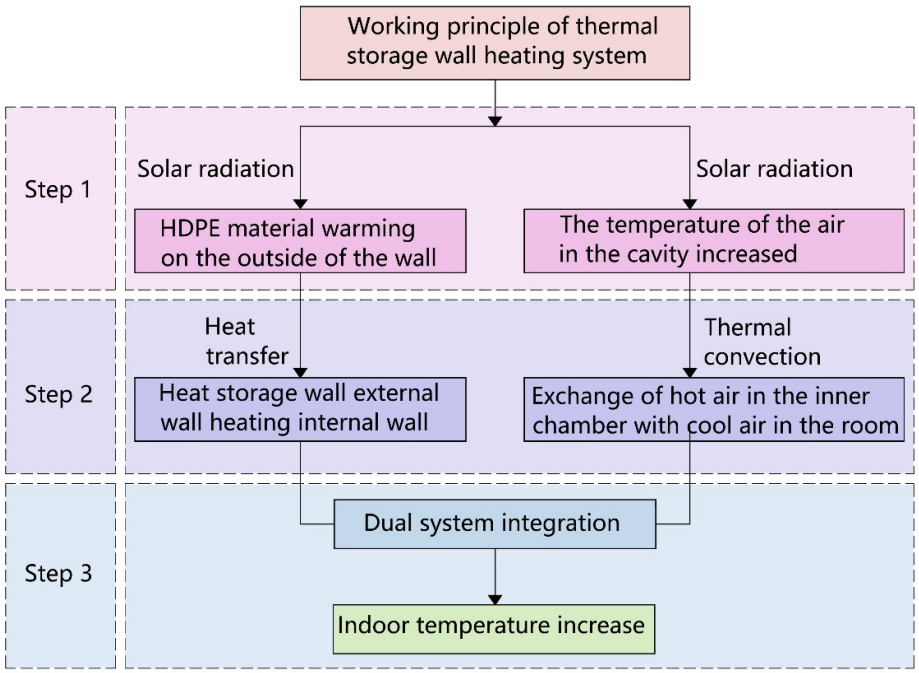


Figure 6. Working principle of TSWHS.

The first step is solar radiation heating the internal air layer and the external HDPE. The principle of the thermal process is based on heating convection and radiation. The heat transfer is majorly transient and follows Planck's law in the process of thermal radiation with the following equation:

$$E_{b\lambda} = \frac{c_1 \lambda^{-5}}{e^{c_2/(\lambda T)} - 1}, \quad (2)$$

where $E_{b\lambda}$ is the blackbody spectral radiation intensity in W/m^3, λ is the wavelength in m. T is the blackbody thermodynamic temperature in K, e is the base of the natural logarithm, c_1 is the first radiative constant with a value of 3.7419×10^{-16} W·m^2, and c_2 is the second radiative constant with a value of 1.4388×10^{-2} m·K.

The second step is HDPE heating the inner wall, with the heat transfer mainly occurring via heat conduction, which is the same as the heat transfer principle in the first step, and the process is solid–solid coupled heat transfer. In this process, Fourier's law is satisfied, and its equation is as follows:

$$q = \frac{\Phi}{A} = -\lambda \frac{dt}{dx}, \quad (3)$$

where q is the heat flow density in w/m^2, Φ is the heat flow rate in W, A is the area in m^2, and x is the axis perpendicular to the area A. λ is the proportionality coefficient, called the thermal conductivity, and "-" indicates that heat transfer is in the direction opposite to the temperature rising direction; dt/dx is the rate of change of the object's temperature along the x-direction.

In the third step, when the temperature of the inner surface of the wall (A in Figure 7) is the same as the outer surface of the wall (B in Figure 7), the TSW raises the entire room temperature mainly via heat transfer in the form of thermal radiation. Simultaneously, the warm air in the TSW is exchanged through vents in the wall with interior cold air, thus raising the room temperature. With thermal convection, Newton's law of cooling is followed:

$$q = h(t_w - t_f). \quad (4)$$

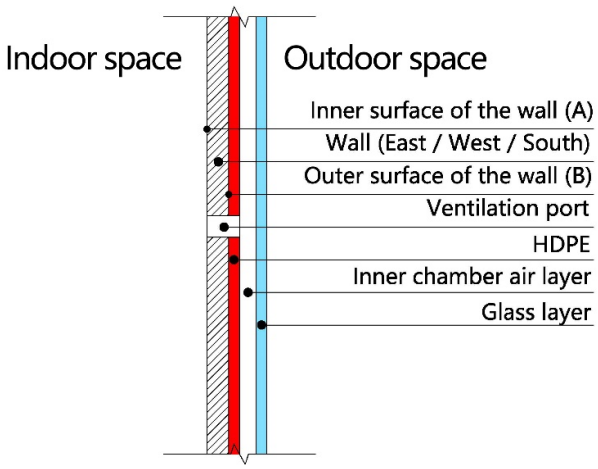


Figure 7. Detailed introduction of TSW.

This equation is used when the fluid is heated, where q is the heat flow density in w/m^2, t_w is the wall temperature and t_f is the fluid temperature in °C, and h is the surface heat transfer coefficient in $w/(m^2 \cdot K)$.

2.2.3. Analysis of OHS

(1) With solar radiation

There are two common ways of heating in Southern Shaanxi where winters are cold. One of these types is passive heating, called OHS, where the heat source is mainly solar radiation and internal heat gains. This method of heating via solar radiation mainly heats the walls via heat conduction to raise the room temperature. The first step is that the outer surface of the wall absorbs heat through solar radiation. The second step is that the inner surface of the wall is heated by the outer surface via heat conduction. The third step is that the release of heat from the inner wall raises the interior temperature through a combination of three types of heat transfer. It is clear that the efficiency of OHS heating is very low, and the internal rise of room temperature is very low. The stabilized temperature is 2.5 °C more compared to the outdoor temperature.

(2) Without solar radiation

The main source of heating for the OHS is mainly internal heat gain without solar radiation. It consists mainly of heat created by various sources of household electricity and stoves. Indoor temperature is also impacted by building size, insulation, and air tightness of materials. Without radiation, the indoor temperature is only impacted by household appliances and stoves, and the variation of indoor temperature is very small, only 0.1 °C above the external temperature.

2.2.4. Analysis of TSWHS

(1) With solar radiation

The absorption and storage capacity of HDPE can increase the internal temperature of residential buildings. HDPE with high heat absorption and storage capacity is added to the exterior walls to absorb, store, and release heat into the room during the daytime when solar radiation is available. It releases heat at night to warm the room. After the TSW absorbs heat, the temperature rises significantly. Specifically, 1 h later, the room temperature increased to 0.7 °C. The maximum temperature of the bedroom reached 8.9 °C at 4:00 p.m. Thus, the house was heated better with HDPE, and the increase in temperature was improved, as was the heating time after using HDPE.

(2) Without solar radiation

The situation was analogous to that of the OHS without solar radiation. The temperature increase in the TSW was slow and very small compared with the external temperature. The interior temperature increased by 0.3 °C. In previous studies, the effect of internal heat gains was less considered. In this study, this factor was added to make the simulation results more accurate.

2.3. Simulation Tools and Parameter Settings

2.3.1. The Application of Simulation Tools

(1) ANSYS

The simulation software used was ANSYS developed by the American company ANSYS, which is a large general finite element analysis software with a broad application range. In this study, the software was mainly used for thermodynamic related simulations, which mainly included two aspects: steady-state and transient thermal calculations, to mainly determine the temperature changes of HDPE on the outer surface of the wall, the inner and outer walls, and the heating time; thermal convection and thermal radiation calculations, to determine the effect of changes in solar radiation on the air temperature inside the glass layer. The temperature change of the TSW and its influence on the interior temperature were also investigated. The objective was to derive the time of heating the room by TSW and the change in room temperature after heating equilibrium by simulation.

(2) EnergyPlus

EnergyPlus was developed by the US DOE and LBNL as energy simulation software. It allows the calculation of the building's cooling and heating loads, as well as the dynamic energy consumption throughout the year, as a function of the physical composition of

the building and the HVAC system. In this study, the software was utilized to compute annual energy depletion, temperature, and duration of thermal comfort. The calculation steps were as follows: to build the model using OpenStudio and import it into EnergyPlus, to enter the data of walls, glass, and other related materials, and to set up the virtual air conditioner for calculating indoor energy consumption and thermal comfort time.

2.3.2. Parameter Setting

(1) Dividing the mesh

First, a new fluid flow board was created in ANSYS, the built model was imported, and each envelope of the building and the internal air were named according to the classification of solid and fluid, respectively. The mesh was then set and divided according to the methodology offered by Arturs et al. The grid setup is very important in the simulation process because it defines the precision of the statistical simulation. Staveckis [57] used five values and 0.34 million hexagons to partition the grid. In this study, the mapping grid and local refinement methods were chosen. The simulation time was managed by setting the grid accuracy.

(2) Calculation conditions

First, the temperature unit was set, and the gravity effect was turned on. Next, the k-epsilon equation was activated and selected, and the RNG buoyancy effect was turned on. The convergence values are crucial for the accuracy of the simulation results: 6–10 for temperature, 10–15 for energy, and 4–10 for other values. Third, the solar radiation equation was activated, and the longitude and latitude information of the study site, as well as the simulation date, was entered. Fourth, commands were entered in the status bar to turn on the ground reflection, diffuse reflection, and reflection values in turn, and to turn on the solar load. Fifth, the material properties were set. Sixth, the calculation domain was opened.

(3) Setting the boundary conditions and calculation

Next, the boundary conditions, including the floor, glass, wall, and fluid, were set. Then, the control items were selected, and the locations to be focused on were marked, before establishing numerical settings and iterative calculation settings. After the setup, the solution calculation was performed.

2.4. Simulation Analysis

The software used was Rhino, EnergyPlus, Ansys, etc. The threshold criterion was turning solar radiation on or off. The steps of the software simulation are described below. Firstly, the model was created with Rhino. Secondly, Ansys was imported to set the parameters, perform the simulation, and obtain the results. Lastly, the thermal load was computed by EnergyPlus. The process consisted of three steps. Firstly, the heating of the OHS was simulated. Secomdly, the heat extraction and exotherm of the TSW were simulated. Thirdly, the appropriate time and the reduction in the thermal payload of TSWHS were simulated. Table 2 shows the building information, and Table 3 shows the properties of the materials.

Table 2. Architectural details of traditional houses and their material types in southern Shaanxi.

Building Detail Name	Material Type
Roof	12 mm thick No. 3 blue tile, 240 mm × 200 mm
TSW outer glass	6 mm glass
TSW insulation	10 mm HDPE
Wall	3 mm lime mortar + 240 mm clay brick masonry + 3 mm lime mortar
Door	45 mm wood
Window	6 mm single-layer glass
floor	100 mm crushed stone, 10 mm cement mortar

Table 3. Physical properties of materials of traditional houses.

Type of Material	Density (kg/m^3)	Thermal Conductivity (W/m·K)	Specific Thermal Capacity (J/kg·K)
Cement/mortar	1800	0.93	1050
Red brick	1700	0.76	1050
Lime/mortar	1600	0.81	1050
Gravel concrete	2300	1.51	920
Wood	500	0.14	2510
Tile	2700	203	920
HDPE	964	0.36	2301

The simulation process of the paper used a single control variable method to verify the energy-saving potential of TSWHS by turning on or off solar radiation. To exclude the influence of other factors on the simulation results, the factor of convection in the air was ignored, and the simulated results remained largely consistent with the measured results; therefore, the problem was also solved by applying this idea in the simulation process.

3. Results and Analysis

3.1. Comparison of OHS and TSWHS without Solar Radiation

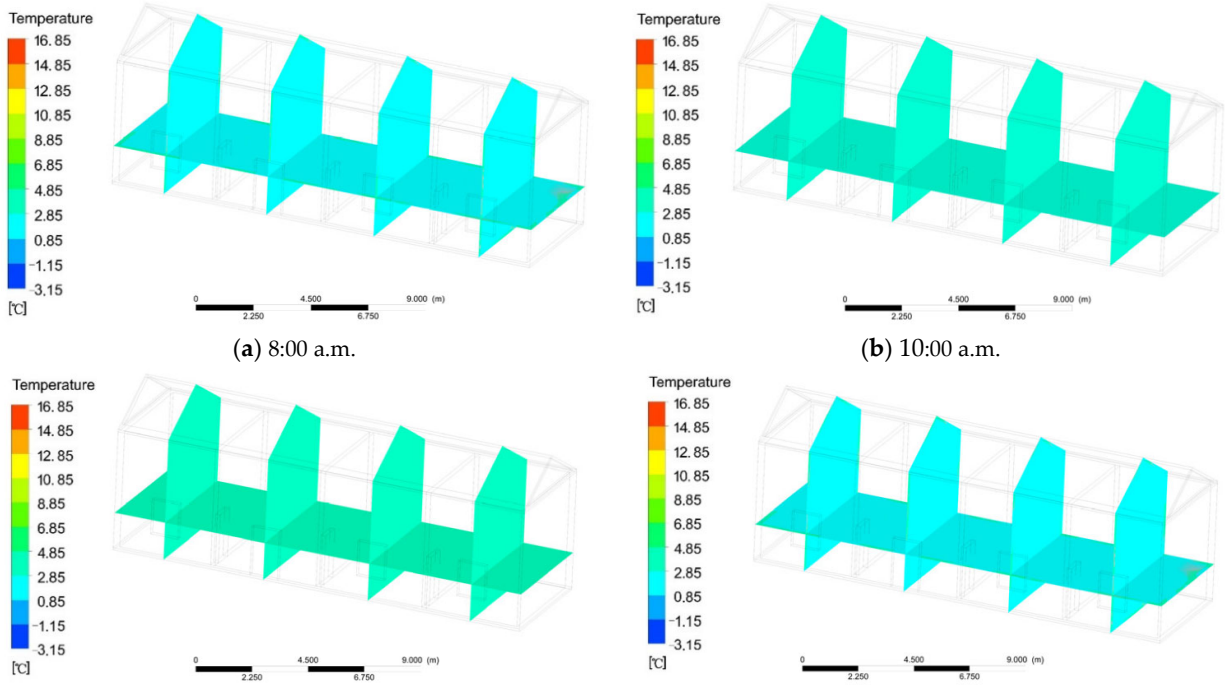
3.1.1. OHS without Solar Radiation

To validate the heating effect of TSWHS without solar radiation, OHS was used as a benchmark for comparison. According to the simulation, the indoor temperature of OHS was not significantly different from the outdoor. The simulated time included daytime and nighttime. In the daytime, the interior temperature was strongly influenced by solar radiation during the period of 8:00 a.m. to 8:00 p.m. Interior temperature was unaffected by solar radiation during nighttime for the period from 8:00 p.m. to 8:00 a.m. This simulated time was used for three heating conditions. Depending on the computed values, the variation of interior temperature was as follows: during the night period from 8:00 p.m. to 8:00 a.m., the temperature gap between inside and outside was small, and the interior temperature is 2.6–3.8 °C. The daytime period was from 8:00 a.m. to 8:00 p.m., where the mean interior temperature was 3.2 °C from 8:00 a.m. to 12:00 p.m. (Figure 8a,b). This is mostly because of the low exterior temperature and the lack of other heat sources indoors. From 12:00 p.m. to 2:00 p.m., the interior temperature was kept constant with an average temperature of 3.3 °C (Figure 8c,d). Both interior and exterior temperatures began to increase slightly from 2:00 p.m. to 5:00 p.m., with the interior temperature stabilizing at 4.2 °C. The external temperature started to decrease, and the interior temperature was 3.6 °C from 5:00 p.m. to 8:00 p.m. Without solar radiation, the average interior temperature of OHS was 3.7 °C, which was not much different from the exterior mean temperature of 0.5 °C.

3.1.2. TSWHS without Solar Radiation

In this case, the temperature gap between the interior and exterior was quite low. TSWHS added a TSW to the exterior walls of the house. On the basis of the OHS model, TSW was added to create TSWHS, and then parameters were set and simulated. The simulation resulted in a temperature of 2.7–3.8 °C at the TSW and a room temperature of 2.9–3.9 °C between 8:00 p.m. and 8:00 a.m. at night. The mean temperature at the TSW was 3.9 °C during the period from 8:00 a.m. to 8:00 p.m. during the day and 3.8 °C during the period from 8:00 a.m. to 10:00 a.m. in the room (Figure 9a,b). The major cause was the very low outside temperature during nighttime, which greatly affected the interior temperature. The TSW had a mean temperature of 4.3 °C. From 12:00 p.m. to 2:00 p.m., the average room temperature remained the same with a value of 4.2 °C (Figure 9b,c). From 2:00 p.m. to 6:00 p.m., indoor household appliances and other heat sources started to be used and the indoor temperature increased slowly. The mean temperature of the TSW was 4.8 °C,

and the mean interior temperature was 4.6 °C (Figure 9c,d). The external temperature commenced to drop between 6:00 p.m. and 8:00 p.m., and the interior temperature dropped accordingly. The mean temperatures of the TSW and the interior were 4.1 °C and 3.9 °C, respectively. Without solar radiation, the internal temperature changed little. The mean temperature of the TSW was 3.8 °C, and the mean interior temperature was 3.7 °C. The average interior temperature was 0.6 °C above the exterior temperature.



(**a**) 8:00 a.m. (**b**) 10:00 a.m.

(**c**) 2:00 p.m. (**d**) 6:00 p.m.

Figure 8. (**a**,**b**) Indoor temperature conditions from 8:00 a.m. to 10:00 a.m.; (**c**,**d**) indoor temperature conditions from 2:00 p.m. to 6:00 p.m.

3.1.3. Comparison Results

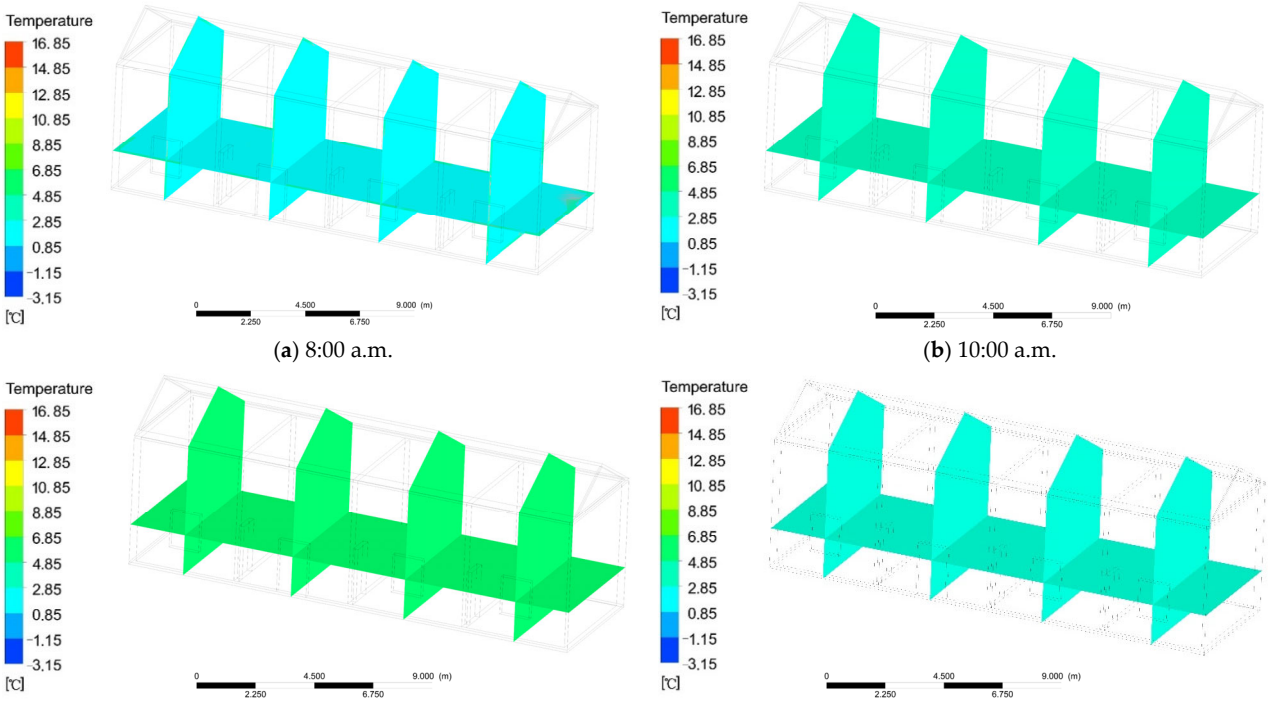
Without solar radiation, the interior temperature of OHS and TSWHS had a very little gap with the exterior temperature. When using OHS, the interior temperature increased by 1.2 °C, and the heating rate is 0.15 °C/h. When using TSWHS, the interior could be raised by 1.3 °C with a heating rate of 0.16 °C/h. This is because, in the absence of solar radiation, the room temperature was mainly affected by the outside, and the heat source was mainly internal heat gains; hence, the heating rate of both heating methods was very inefficient, and the improvement of interior temperature was limited.

3.2. Comparison of OHS and TSWHS with Solar Radiation

3.2.1. OHS with Solar Radiation

The OHS relied heavily on solar radiation. Simulation conditions and parameter settings were consistent with the case without solar radiation. From 8:00 a.m.to 12:00 p.m., the temperature of the room increased sequentially from east to west, from the initial 3.5 °C to 5.8 °C, as the altitude angle of the sun changed. Since the west side of the room received less solar radiation, the temperature increased less (Figure 10a,b). The range of variation in the room temperature was small, and the room temperature tended to be stable from 12:00 p.m. to 2:00 p.m., with an average room temperature of 5.5 °C (Figure 10c,d). The western side of the building received more solar radiation from 2:00 p.m. to 8:00 p.m. The west side of the room reached the highest temperature of 5.8 °C at 3:00 p.m., and then the temperature slowly decreased (Figure 10e,f). At this time, the east side of the building received less solar radiation, and the interior temperature decreased from 5.7 °C to 3.8 °C.

The graph shows that, when solar radiation was available, the average indoor temperature at OHS was 5.6 °C, which was 2.5 °C higher than the exterior temperature.



(**a**) 8:00 a.m. (**b**) 10:00 a.m.

(**c**) 2:00 p.m. (**d**) 6:00 p.m.

Figure 9. (**a**,**b**) Indoor temperature conditions from 8:00 a.m. to 10:00 a.m.; (**c**,**d**) indoor temperature conditions from 2:00 p.m. to 6:00 p.m.

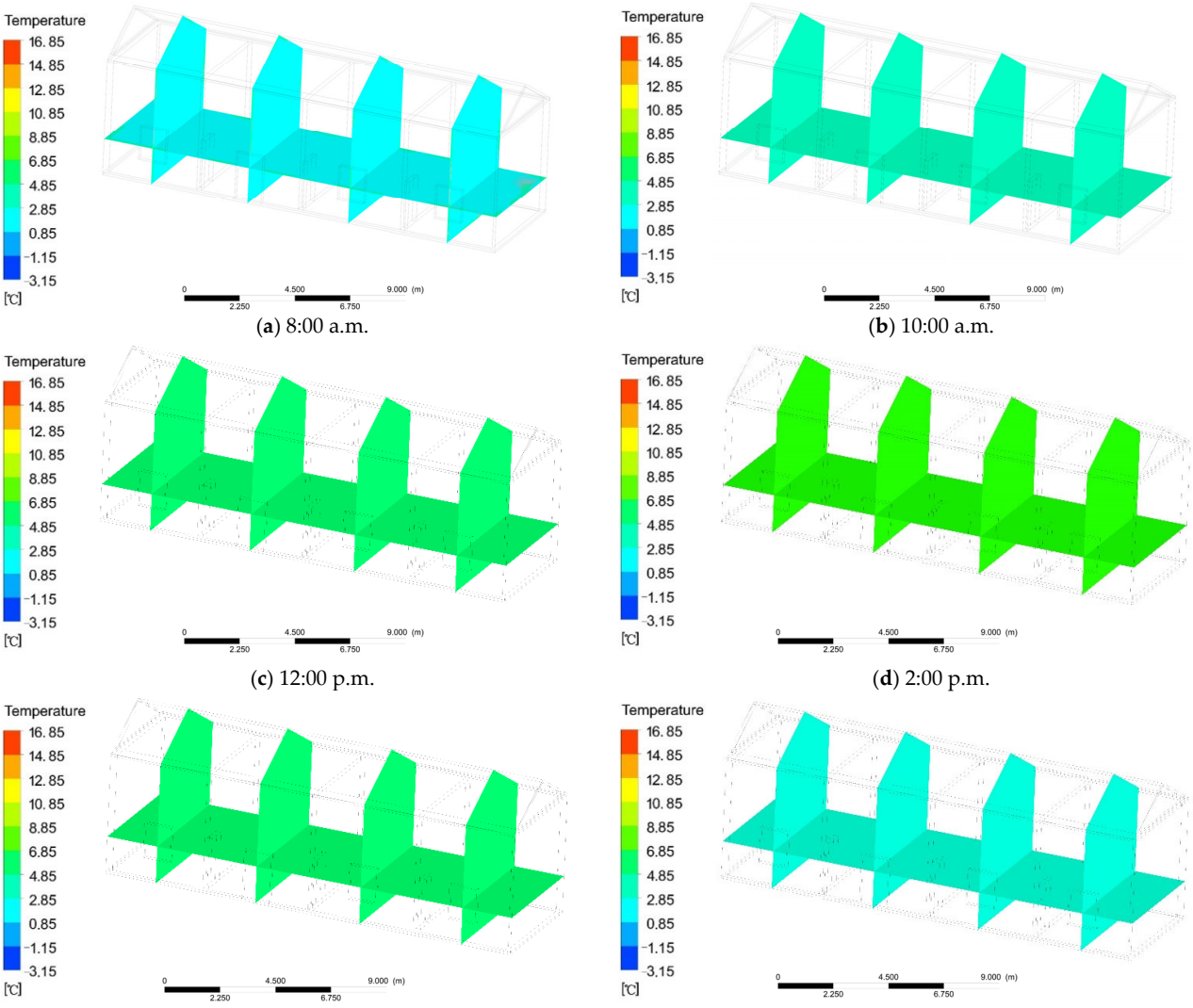
3.2.2. TSWHS with Solar Radiation

To validate the heating efficiency of the TSWHS, the simulation results of the OHS were used as a basis for comparison. The preliminary interior temperature was 3.1 °C. The heating process of the TSW was divided into three steps. Firstly, when solar radiation is available, the HDPE temperature and the air temperature inside the glass rise. Secondly, the HDPE heats the inner wall via heat conduction. Lastly, the interior wall temperature rises, thus heating the room. Meanwhile, the hot air inside the TSW flows into the room, raising the room temperature through a double action.

Step 1 was solar radiation heating the HDPE and air in the glass layer. The variation of temperature in each direction of the building was slightly different due to the difference of the angle of solar radiation. At 8:00 a.m., the air inside the HDPE and glass layers was heated. The TSW temperature increased in a stepwise manner from east to west.

To study the temperature evolution of HDPE, the cross-sectional temperature was chosen for the study. The temperature change is such that the temperature of HDPE after receiving solar radiation changes during the day as a result of the change in the azimuth of the sun and the duration of the thermal radiation. The height of the cross-section is 1.5 m above the ground, which is consistent with the height of the human activity space in the room. HDPE was added to the outside of the three side walls of the house at the locations shown in Figure 11a. The temperature variation of HDPE is shown in Figure 11b. The simulation started at 8:00 a.m. with an initial temperature of 3.5 °C. At 9:00 a.m., the temperatures were 12.4 °C, 6.8 °C, and 4.6 °C on the east, central, and west sides, respectively. At 10:00 a.m., the temperatures on the east, middle, and west sides were 22.1 °C, 14.4 °C, and 10.3 °C. At 11:00 a.m., the temperatures on the east, middle, and west sides were 30.4 °C, 23.5 °C, and 19.8 °C. The temperature achieved the maximum value of 32.0 °C at 12:00 p.m. From 12:00 p.m. to 2:00 p.m., the temperature of the TSW was kept at 32.0 °C. From 2:00 p.m. to 4:00 p.m., the temperature started to drop, and the sun

was on the west side of the room; thus, the temperature of the TSW on the west side was higher than the temperature on the east side. The temperatures of the three parts of the TSW were 25.3 °C, 26.8 °C, and 27.6 °C respectively. At 5:00 p.m., the temperatures in the eastern, central, and western rooms were 12.3 °C, 14.8 °C, and 17.4 °C, respectively. At 6:00 p.m., the temperatures of the three sections were 7.6 °C, 10.7 °C, and 13.3 °C, respectively. At 7:00 p.m., the temperatures of the three sections were 4.8 °C, 8.1 °C, and 10.3 °C. The temperature was 3.6 °C at 8:00 p.m. From 8:00 p.m. to 8:00 a.m. the next day, the temperature of the TSW remained the same as the external temperature, which was 3.6 °C. The trend of change in the three parts was the same, and the time of the rising phase became longer. The eastern wall was the first to receive solar radiation, followed by the central wall, and finally the western wall. The trend of change was the same when the temperature was stable. The decreasing trend of temperature became steeper in turn, which was the opposite of the rising phase.



(**a**) 8:00 a.m. (**b**) 10:00 a.m.

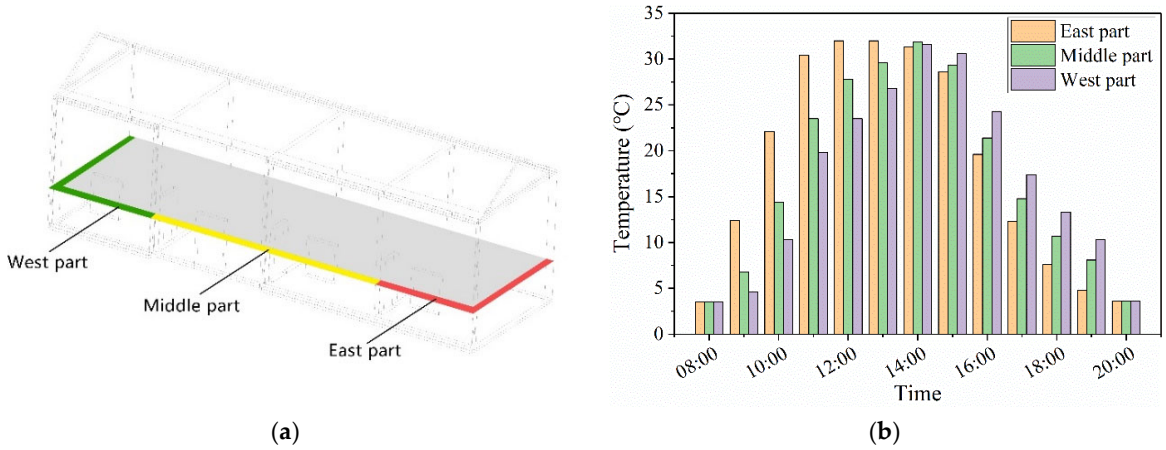
(**c**) 12:00 p.m. (**d**) 2:00 p.m.

(**e**) 4:00 p.m. (**f**) 6:00 p.m.

Figure 10. (**a**,**b**) Indoor temperature conditions from 8:00 a.m. to 10:00 a.m.; (**c**,**d**) indoor temperature conditions from 12:00 p.m. to 2:00 p.m.; (**e**,**f**) indoor temperature conditions from 4:00 p.m. to 6:00 p.m.

Step 2 was the heat transfer from the TSW itself. The principle is that HDPE heated the surface of the exterior wall. After simulation, the temperature of HDPE continued rising from 8:00 a.m. to 12:00 p.m. At 1:00 p.m., the temperature of the TSW reached the highest value of 31.6 °C. From 12:00 p.m. to 3:00 p.m., the temperature of the TSW stayed the same

at 31.6 °C. From 3:00 p.m. to 8:00 p.m., the temperature of the TSW started to drop, and, at 8:00 p.m., the temperature of the TSW was 3.3 °C. From 8:00 p.m. to 8:00 a.m. the next day, the temperature of the TSW was 3.3 °C.



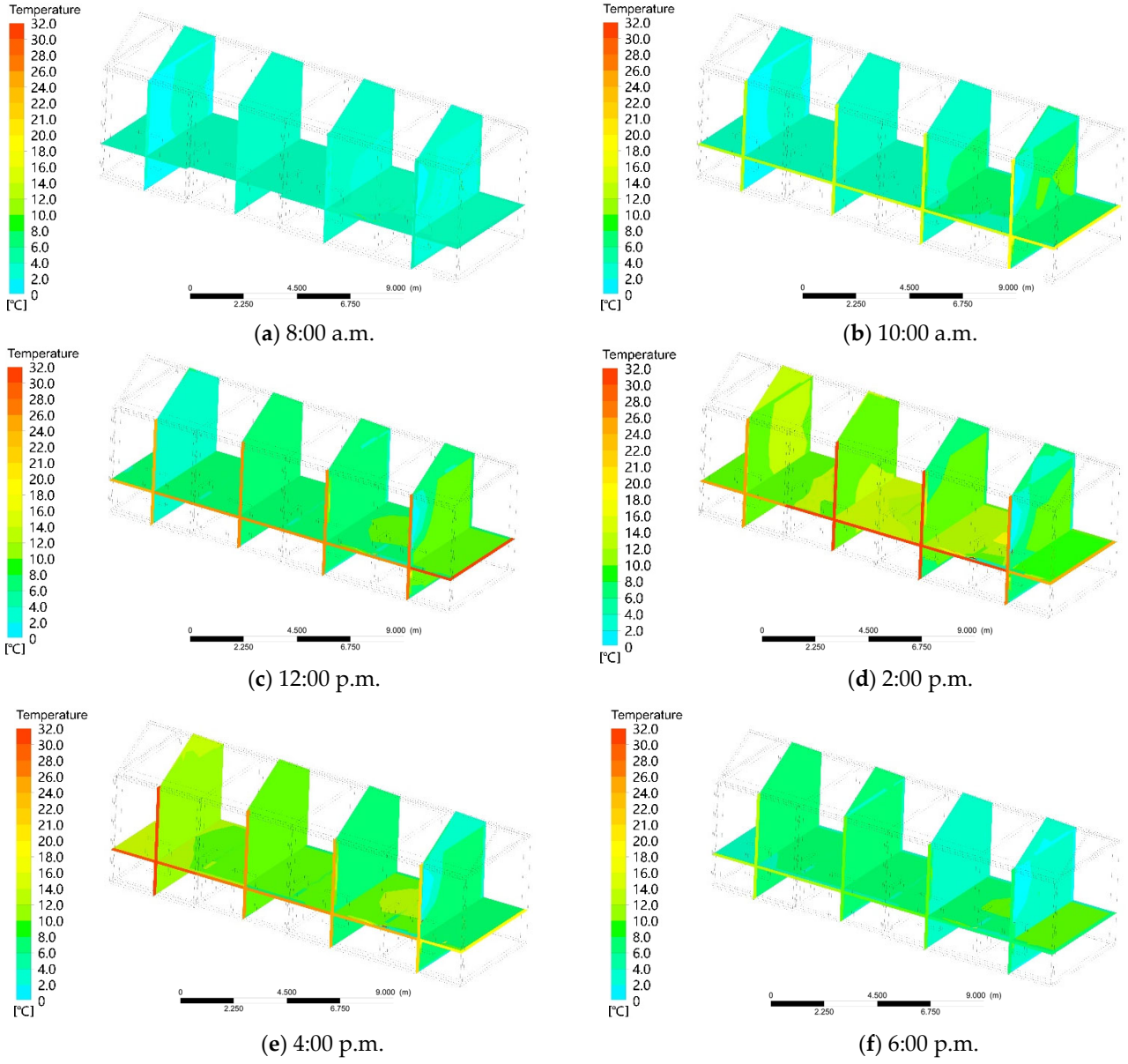
(**a**) (**b**)

Figure 11. (**a**) Location of HDPE for TSW; (**b**) temperature change of the three parts of HDPE for TSW.

Step 3 was the interior wall heating the room, and the hot air inside the glass flowing indoors. The interior temperature changes for 24 h were as follows: at 8:00 a.m., the indoor temperature was 3.5 °C, which was the same as that of the TSW (Figure 12a). At 9:00 a.m., the indoor temperatures in the three sections were 5.2 °C, 4.4 °C, and 3.9 °C, respectively. At 10:00 a.m., the indoor temperatures in the east, middle, and west sections were 5.9 °C, 4.7 °C, and 4.3 °C, respectively (Figure 12b). At 11:00 a.m., the indoor temperatures in the three sections were 6.3 °C, 5.2 °C, and 4.6 °C, respectively. At 12:00 p.m., the indoor temperatures in the three sections were 6.9 °C, 6.1 °C, and 5.5 °C, respectively (Figure 12c). At 1:00 p.m., the indoor temperatures in the three sections were 7.8 °C, 6.9 °C, and 6.2 °C, respectively. At 2:00 p.m., the indoor temperatures in the three sections were 8.3 °C, 9.0 °C, and 8.4 °C (Figure 12d). At 3:00 p.m., the indoor temperatures in the three sections were 8.3 °C, 9.0 °C, and 8.4 °C. At 4:00 p.m., the indoor temperatures in the three sections were 8.2 °C, 8.7 °C, and 9.1 °C (Figure 12e). At 5:00 p.m., the indoor temperatures in the three sections were 7.5 °C, 7.6 °C, and 8.4 °C. At 6:00 p.m., the indoor temperatures in the three sections were 5.2 °C, 5.9 °C, and 6.4 °C (Figure 12f). At 7:00 p.m., the indoor temperatures in the three sections were 4.7 °C, 5.2 °C, and 5.6 °C. At 8:00 p.m., the indoor temperatures in the three sections were 3.4 °C, 3.5 °C, and 3.6 °C. The interior temperature was maintained at 3.5 °C from 8:00 a.m. to 8:00 p.m. the next day, the same as the exterior temperature.

3.2.3. Comparison Results

TSWHS is a new green heating system that saves energy and has a good heating effect. TSWHS starts working during the day with solar radiation. The initial indoor temperature was 3.5 °C. After being influenced by solar radiation, the indoor temperature started to rise at 9:00 a.m. with a mean temperature of 4.5 °C. Because of the different amounts of solar radiation received by the three sections of the room, it showed different temperatures. At 3:00 p.m., the temperature of the central room reached a maximum value of 9.1 °C, and the average temperature of the three parts of the room was 8.6 °C. The indoor temperature started to drop at 5:00 p.m. with an average indoor temperature of 7.8 °C. The temperature increased by 5.1 °C with an average heating efficiency of 0.64 °C/h. OHS mainly relies on solar radiation heat generation from the walls to influence the indoor temperature; the temperature increased by 2.3 °C with an average heating efficiency of 0.29 °C/h. The TSW heating improved the heating rate and duration effectively compared to the OHS.



(**a**) 8:00 a.m. (**b**) 10:00 a.m.

(**c**) 12:00 p.m. (**d**) 2:00 p.m.

(**e**) 4:00 p.m. (**f**) 6:00 p.m.

Figure 12. (**a**,**b**) Indoor temperature conditions from 8:00 a.m. to 10:00 a.m.; (**c**,**d**) indoor temperature conditions from 12:00 p.m. to 2:00 p.m.; (**e**,**f**) indoor temperature conditions from 4:00 p.m. to 6:00 p.m.

3.3. Usage Time of TSWHS

According to the Chinese building industry design standard [51], the indoor thermal comfort temperature of houses in HSCW zones in winter is defined as higher than 18 °C. Accordingly, this study used 18 °C as the standard value to measure the total time of interior temperature above 18 °C after adopting the TSWHS, to evaluate the TSWHS heating and energy efficiency. According to the climatic conditions in southern Shaanxi, the heating time of the TSWHS is concentrated from October to March of the next year. Using EnergyPlus simulation, the use effect of the TSWHS and OHS was evaluated. The results are presented below. The OHS was used in solar radiation for 1023 h, corresponding to 11.68% of the year. The time of TSWHS usage was 1332 h, accounting for 15.21% of the whole year (Figure 13).

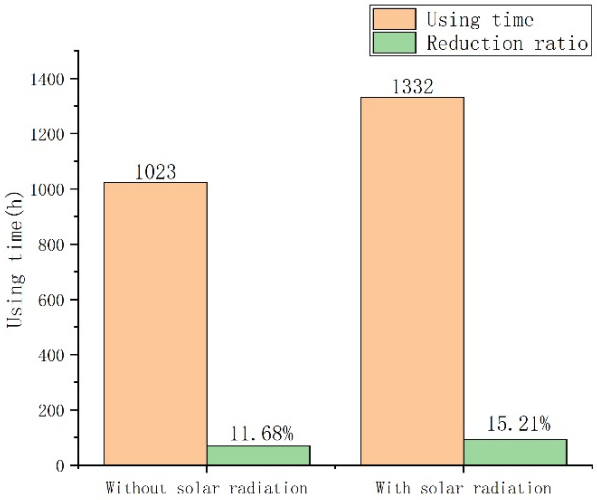
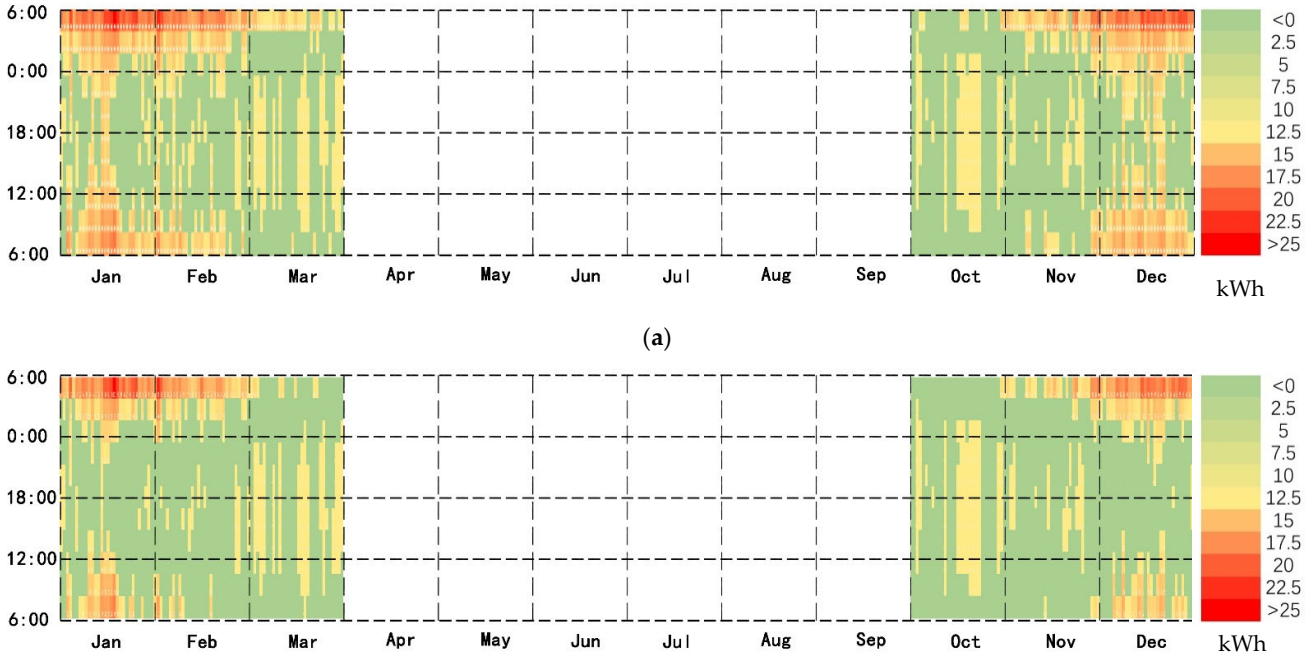


Figure 13. Usage time of TSWHS.

3.4. Analysis of Energy Saving of TSWHS

The annual thermal payload of the house with TSWHS and OHS was calculated using EnergyPlus software simulation, and the result was that the annual thermal payload of the house with OHS with solar radiation was reduced to 625.36 kWh with a reduced rate of 9.87% (Figure 14a). With solar radiation, the annual thermal payload of the house with TSWHS was decreased to 1726.43 kWh with a reduction rate of 27.24% (Figure 14b).



(**a**)

(**b**)

Figure 14. (**a**) Energy consumption of OHS; (**b**) energy consumption of TSWHS.

3.5. Thermal Comfort Analysis of TSWHS

The indoor thermal comfort conditions for OHS and TSWHS with and without solar radiation were obtained through EnergyPlus simulations. Using 18 °C as a standard value for thermal comfort in residential buildings [51], the total number of hours below 18 °C throughout the year with TSWHS was calculated, and the advantage of TSWHS was derived by comparing it with the OHS system. Without solar radiation, with the

OHS system, the total annual time when the indoor temperature was lower than 18 °C was 4806 h, corresponding to 54.87% of the total annual time (Figure 15a). Without solar radiation, with the TSWHS, the total annual time when the indoor temperature was lower than 18 °C was 3929 h, corresponding to 44.85% of the total annual time (Figure 15b). With the TSWHS, the total annual time when the indoor temperature was below 18 °C was 3645 h with solar radiation, corresponding to 41.61% of the total annual time (Figure 15c).

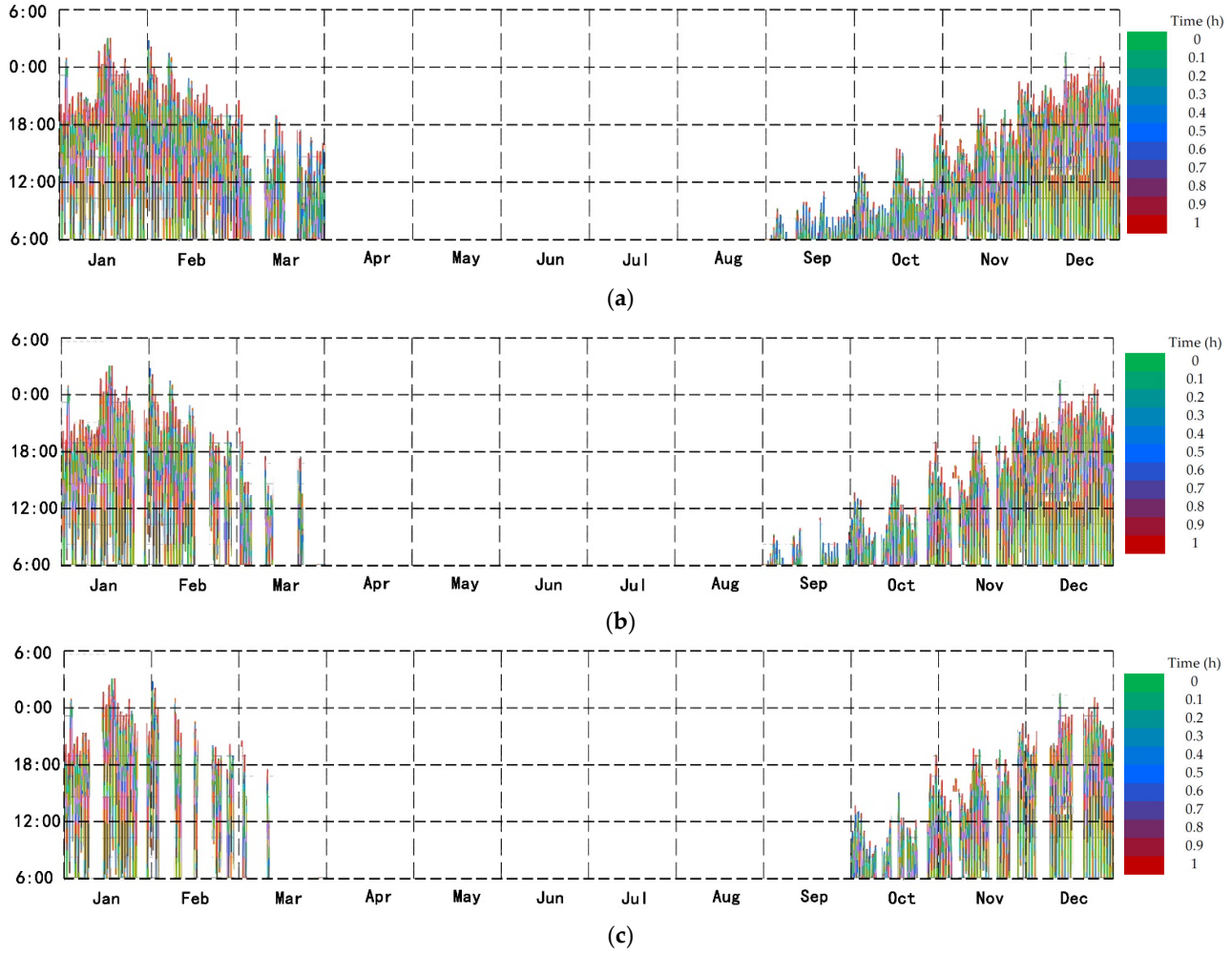


Figure 15. (**a**) Analysis of the time below 18 °C with OHS without solar radiation; (**b**) analysis of the time below 18 °C with TSWHS without solar radiation; (**c**) analysis of the time below 18 °C with TSWHS with solar radiation.

4. Discussion

Proper use of solar energy for warming can be effective in reducing building energy depletion. In addition, the thermal retention performance of the enclosure is also an essential factor affecting energy efficiency, as well as the effectiveness of indoor heating. This work proposed TSWHS for houses in HSCW, using solar energy for interior heating and installing HDPE insulation, a glazing layer on the outside of the walls, and vents in the exterior walls. Through the use of insulation and heat storage of PCMs, the greenhouse effect of the glass layers, and the exchange of hot air inside the glass interlayer with cold indoor air through the vents, the room temperature and the effective energy saving could be enhanced. To verify the heating effectiveness and energy consumption of TSWHS, TSWHS and OHS were compared by setting the presence or absence of solar radiation as a boundary condition to prove the effectiveness of TSWHS. Previous studies focused more on passive designs, such as solar chimneys, Trumbell walls, and air-source heat pumps, or

they focused on studying the insulation properties of the envelope. To improve the thermal capacity and to solve the limitations of previous studies, passive design was studied along with the thermal performance of the envelope to further improve heating effectiveness and energy efficiency. The results of this study could provide a method for winter heating and energy saving in conventional houses in cold winter areas.

There are still some shortcomings in this study; the cost factors of HDPE and large-area glass were less considered when building retrofitting was carried out. The ease of construction in practice was also not considered, but these factors do not affect the simulation results and can be solved by technical means. In the simulation setup, the starting temperature was assumed to be a fixed value, and the effect of air convection on the room temperature was ignored. However, these factors do exist in reality. In future research, these factors should be further considered, and, by comparing the thermal insulation performance and cost of different materials, a suitable material should be chosen through a practical situation.

5. Conclusions

The challenge and the opportunity for passive heating with TSWs include addressing the problem of cold indoor winter homes and excessive energy consumption in southern Shaanxi, while the region has excellent potential for solar radiation. Considering the lack of passive heating design in traditional buildings, the use of solar energy for heating can effectively raise indoor temperatures and save energy. Meanwhile, the thermal insulation of the building envelope and the insulation measures are the most important factors influencing the interior temperature. The innovation of this work was to design a TSWHS that simultaneously achieves daytime heat storage heating, nighttime heat release and extended heating time, and hot air flow indoors. The heating conditions of OHS and TSWHS were simulated and evaluated using ANSYS and EnergyPlus software, respectively, in terms of usage time, temperature gain, and energy-saving capacity. The study findings are detailed below.

1. A new TSWHS was proposed. By installing HDPE material on the outside of the east, west, and south walls of the residential building, the temperature of the HDPE of the TSW increased to heat the room through heat conduction when solar radiation was available. Therefore, heat could be absorbed during the day, while exothermic heat led to hot air flow indoors at night, extending the time of TSWHS heating.

2. A practice of adding a glass interlayer outside the wall was proposed, such that the glass and the wall constituted a confined space, using the principle of the sunlight between the greenhouse, whereby the air temperature inside the glass interlayer rose together with HDPE to heat the room so that the indoor temperature was further increased.

3. Ventilation openings were opened at the top and bottom of the east–west and south exterior walls to make the hot air inside the interlayer exchange with the cold air inside, thereby enhancing the indoor temperature.

4. In the research analysis, the presence or absence of solar radiation was proposed as the boundary condition for ANSYS and Energyplus analysis to verify the effectiveness of the TSWHS in terms of heating and energy saving. By comparing TSWHS with OHS, the year-round usage time of the TSWHS and the energy savings were discussed in detail. The results were that, with solar radiation, the temperature increase with TSWHS was 5.1 °C, which was 1.6 times higher than the OHS system. The annual usage time with TSWHS was 1332 h, reflecting a 30% improvement compared to OHS. The annual heat load of TSWHS was reduced by 1726.43 kWh, corresponding to a 1.8 times improvement in energy saving compared to OHS. The annual time below 18 °C using TSWHS was 3645 h, i.e., 24.16% lower compared to OHS.

Author Contributions: Conceptualization, S.C.; methodology, S.C., S.Y. and B.J.D.; software, S.C. and W.M.; investigation, S.C., J.C. and J.M.; writing—original draft preparation, S.C.; writing—review and editing, S.C. All authors have read and agreed to the published version of the manuscript.

Funding: This study was funded by the Ankang University Education Teaching Reform Research Project in 2022 (No. JG202225) and the Shaanxi Provincial Department of Education Special Project (No. 21JK0007).

Institutional Review Board Statement: Not applicable.

Informed Consent Statement: Informed consent was obtained from all subjects involved in the study.

Data Availability Statement: Not applicable.

Acknowledgments: The authors thank all the professors and students who helped with this study.

Conflicts of Interest: The authors declare no conflict of interest.

References

1. International Energy Agency (IEA). IEA Online Data Services. Available online: https://www.iea.org/data-and-statistics/data-browser/?country=WORLD&fuel=Energy%20consumption&indicator=CO2Industry (accessed on 20 February 2021).
2. Nian, V.; Mignacca, B.; Locatelli, G. Policies toward net-zero: Benchmarking the economic competitiveness of nuclear against wind and solar energy. *Appl. Energy* **2022**, *320*, 119275. [CrossRef]
3. Zhang, Q.; Chen, W.; Ling, W. Policy optimization of hydrogen energy industry considering government policy preference in China. *Sustain. Prod. Consum.* **2022**, *33*, 890–902. [CrossRef]
4. Wang, Z.; Wang, Y.; Huang, F.; Shuai, C.; Li, J.; Ding, L.; Cheng, X. The environmental impact of household domestic energy consumption in rural areas: Empirical evidence from China's photovoltaic poverty alleviation regions. *Sustain. Prod. Consum.* **2022**, *30*, 1019–1031. [CrossRef]
5. Li, Y.; Zhou, T.; Wang, Z.; Li, W.; Zhou, L.; Cao, Y.; Shen, Q. Environment improvement and energy saving in Chinese rural housing based on the field study of thermal adaptability. *Energy Sustain. Dev.* **2022**, *71*, 315–329. [CrossRef]
6. Liu, C.; Xu, M. Characteristics and Influencing Factors on the Hollowing of Traditional Villages—Taking 2645 Villages from the Chinese Traditional Village Catalogue (Batch 5) as an Example. *Int. J. Environ. Res. Public Health* **2021**, *18*, 12759. [CrossRef]
7. Long, H.; Liu, Y.; Wu, X.; Dong, G. Spatio-temporal dynamic patterns of farmland and rural settlements in Su–Xi–Chang region: Implications for building a new countryside in coastal China. *Land Use Policy* **2009**, *26*, 322–333. [CrossRef]
8. Li, Q.; Hu, H.; Ma, L.; Wang, Z.; Arıcı, M.; Li, D.; Luo, D.; Jia, J.; Jiang, W.; Qi, H. Evaluation of energy-saving retrofits for sunspace of rural residential buildings based on orthogonal experiment and entropy weight method. *Energy Sustain. Dev.* **2022**, *70*, 569–580. [CrossRef]
9. Zhou, Q.; Liu, Y.; Qu, S. Emission effects of China's rural revitalization: The nexus of infrastructure investment, household income, and direct residential CO_2 emissions. *Renew. Sustain. Energy Rev.* **2022**, *167*, 112829. [CrossRef]
10. Pozas, B.; Gamero, I.; Domínguez, A.; Castro, P. A methodology to improve energy efficiency and comfort conditions with low-cost ICTs in rural public buildings. *Sustain. Cities Soc.* **2020**, *60*, 102156. [CrossRef]
11. Elaouzy, Y.; Fadar, A. Energy, economic and environmental benefits of integrating passive design strategies into buildings: A review. *Renew. Sustain. Energy Rev.* **2022**, *167*, 112828. [CrossRef]
12. Sun, M.; Han, C.; Nie, Q.; Xu, J.; Zhang, F.; Zhao, Q. Understanding building energy efficiency with administrative and emerging urban big data by deep learning in Glasgow. *Energy Build.* **2020**, *273*, 112331. [CrossRef]
13. Qiao, X.; Kong, X.; Fan, M. Phase change material applied in solar heating for buildings: A review. *J. Energy Storage* **2022**, *55*, 105826. [CrossRef]
14. Qiu, G.; Yu, S.; Cai, W. A novel heating strategy and its optimization of a solar heating system for a commercial building in term of economy. *Energy* **2021**, *221*, 119773. [CrossRef]
15. Xu, W.; Guo, H.; Ma, C. An active solar water wall for passive solar greenhouse heating. *Appl. Energy* **2022**, *308*, 118270. [CrossRef]
16. Wang, Q.; Zhang, G.; Wu, Q.; Shi, L. Solar chimney performance in buildings under three heating modes: An empirical analysis. *Sustain. Energy Technol. Assess.* **2022**, *52*, 102222. [CrossRef]
17. Fan, R.; Li, Y.; Bu, T.; Sun, K.; Zhou, Y.; Shi, J.; Zhang, X. Comparative study of solar hot air heating systems with phase change materials in plateau areas. *Energy Build.* **2020**, *224*, 110265. [CrossRef]
18. Zhang, R.; Wang, D.; Liu, Y.; Chen, Y.; Fan, J.; Song, C.; Wang, Y. Economic optimization of auxiliary heat source for centralized solar district heating system in Tibetan Plateau, China. *Energy Convers. Manag.* **2021**, *243*, 114385. [CrossRef]
19. Elmetwalli, A.; Darwesh, M.; Amer, M.; Ghoname, M. Influence of solar radiation and surrounding temperature on heating water inside solar collector tank. *J. Energy Storage* **2022**, *47*, 103648. [CrossRef]
20. Liu, C.; Han, W.; Wang, Z.; Zhang, N.; Kang, Q.; Liu, M. Proposal and assessment of a new solar space heating system by integrating an absorption-compression heat pump. *Appl. Energy* **2021**, *294*, 116966. [CrossRef]
21. Chi, F.; Wang, R.; Wang, Y. Integration of passive double-heating and double-cooling system into residential buildings (China) for energy saving. *Sol. Energy* **2021**, *225*, 1026–1047. [CrossRef]
22. Wang, X.; Mai, X.; Lei, B.; Bi, H.; Zhao, B.; Mao, G. Collaborative optimization between passive design measures and active heating systems for building heating in Qinghai-Tibet plateau of China. *Renew. Energy* **2020**, *147*, 683–694. [CrossRef]

23. Aksoy, U.; Inalli, M. Impacts of some building passive design parameters on heating demand for a cold region. *Build. Environ.* **2006**, *41*, 1742–1754. [CrossRef]
24. Brown, S.; Morrison, I. Characterizing the performance of a passive solar house with hydronic floor energy capture system—Heating season experiments. *Energy Build.* **2006**, *252*, 111404. [CrossRef]
25. Givoni, B. Characteristics, design implications, and applicability of passive solar heating systems for buildings. *Sol. Energy* **1991**, *47*, 425–435. [CrossRef]
26. Wang, S.; Liu, Y.; Cao, Q.; Li, H.; Yu, Y.; Yang, L. Applicability of passive design strategies in China promoted under global warming in past half century. *Build. Environ.* **2021**, *195*, 107777. [CrossRef]
27. Kuşkaya, S. Residential solar energy consumption and greenhouse gas nexus: Evidence from Morlet wavelet transforms. *Renew. Energy* **2022**, *192*, 793–804. [CrossRef]
28. Wang, D.; Chen, R.; Zhou, Y.; Wang, Y.; Liu, Y. Optimization and techno-economic analysis of combined gas-fired boiler and solar heating system for capacity-increase cities. *Sol. Energy* **2022**, *243*, 225–235. [CrossRef]
29. Gao, D.; Zhao, B.; Kwan, T.; Hao, Y.; Pei, G. The spatial and temporal mismatch phenomenon in solar space heating applications: Status and solutions. *Appl. Energy* **2022**, *321*, 119326. [CrossRef]
30. He, Z.; Farooq, A.S.; Guo, W.; Zhang, P. Optimization of the solar space heating system with thermal energy storage using data-driven approach. *Renew. Energy* **2022**, *190*, 764–776. [CrossRef]
31. Feng, G.; Wang, G.; Li, Q.; Zhang, Y.; Li, H. Investigation of a solar heating system assisted by coupling with electromagnetic heating unit and phase change energy storage tank: Towards sustainable rural buildings in northern China. *Sustain. Cities Soc.* **2022**, *180*, 103449. [CrossRef]
32. Ménard, R.; Souviron, J. Passive solar heating through glazing: The limits and potential for climate change mitigation in the European building stock. *Energy Build.* **2020**, *228*, 110400. [CrossRef]
33. Liu, Z.; Wu, D.; He, B.; Wang, Q.; Yu, H.; Ma, W.; Jin, G. Evaluating potentials of passive solar heating renovation for the energy poverty alleviation of plateau areas in developing countries: A case study in rural Qinghai-Tibet Plateau, China. *Sol. Energy* **2019**, *187*, 95–107. [CrossRef]
34. Dabaieh, M.; Elbably, A. Ventilated Trombe wall as a passive solar heating and cooling retrofitting approach; A low-tech design for off-grid settlements in semi-arid climates. *Sol. Energy* **2015**, *122*, 820–833. [CrossRef]
35. Zhang, X.; Nie, S.; He, M.; Wang, J. Energy-saving renovation of old urban buildings: A case study of Beijing. *Case Stud. Therm. Eng.* **2021**, *28*, 101632. [CrossRef]
36. Mi, P.; Zhang, J.; Han, Y.; Guo, X. Study on energy efficiency and economic performance of district heating system of energy saving reconstruction with photovoltaic thermal heat pump. *Energy Convers. Manag.* **2021**, *247*, 114677. [CrossRef]
37. Kalbasi, R. Usefulness of PCM in building applications focusing on envelope heat exchange—Energy saving considering two scenarios. *Sustain. Energy Technol. Assess.* **2022**, *50*, 101848. [CrossRef]
38. Tadeu, S.; Rodrigues, C.; Marques, P.; Freire, F. Eco-efficiency to support selection of energy conservation measures for buildings: A life-cycle approach. *J. Build. Eng.* **2022**, *61*, 105142. [CrossRef]
39. Wang, Z.; Liu, Q.; Zhang, B. What kinds of building energy-saving retrofit projects should be preferred? Efficiency evaluation with three-stage data envelopment analysis (DEA). *Renew. Sustain. Energy Rev.* **2022**, *161*, 112392. [CrossRef]
40. Wang, Z.; Chen, H.; Sun, X.; Lu, H.; Wang, T. Optimizing the solar-air hybrid source heat pump heating system based on the particle swarm algorithm. *Energy Rep.* **2022**, *8*, 379–393. [CrossRef]
41. Bakos, G. Energy management method for auxiliary energy saving in a passive-solar-heated residence using low-cost off-peak electricity. *Energy Build.* **2000**, *31*, 237–241. [CrossRef]
42. Sun, D.; Wang, L. Research on heat transfer performance of passive solar collector-storage wall system with phase change materials. *Energy Build.* **2000**, *119*, 183–188. [CrossRef]
43. Chandel, S.; Sarkar, A. Performance assessment of a passive solar building for thermal comfort and energy saving in a hilly terrain of India. *Energy Build.* **2015**, *86*, 873–885. [CrossRef]
44. Athienitis, A.K. Investigation of thermal performance of a passive solar building with floor radiant heating. *Sol. Energy* **1997**, *61*, 337–345. [CrossRef]
45. Badescu, V.; Laaser, N.; Crutescu, R.; Crutescu, M.; Dobrovicescu, A.; Tsatsaronis, G. Modeling, validation and time-dependent simulation of the first large passive building in Romania. *Renew. Energy* **2011**, *36*, 142–157. [CrossRef]
46. Arkar, C.; Šuklje, T.; Vidrih, B.; Medved, S. Performance analysis of a solar air heating system with latent heat storage in a lightweight building. *Applied Therm. Eng.* **2016**, *95*, 281–287. [CrossRef]
47. Stevanovic, S. Optimization of passive solar design strategies: A review. *Sustain. Energy Rev.* **2013**, *25*, 177–196. [CrossRef]
48. Li, L.; Chen, G.; Zhang, L.; Zhou, J. Research on the application of passive solar heating technology in new buildings in the Western Sichuan Plateau. *Energy Rep.* **2021**, *7*, 906–914. [CrossRef]
49. Zhou, S.; Razaqpur, A.G. Efficient heating of buildings by passive solar energy utilizing an innovative dynamic building envelope incorporating phase change material. *Renew. Energy* **2022**, *197*, 305–319. [CrossRef]
50. Guo, M.; Liu, Y.; Chen, Y.; Gao, W.; Wang, D.; Tang, H.; Liu, H. Study on the effect of different types and distribution ratio of heat users on operation performance of the distributed solar centralized heating system. *Energy Build.* **2022**, *270*, 112265. [CrossRef]
51. Ministry of Housing and Urban-Rural Development of the People's Republic of China. *Design Standard for Energy Efficiency of Residential Buildings in Hot Summer and Cold Winter Zones*, 1st ed.; China Architecture & Building Press: Beijing, China, 2010; p. 3.

52. Zhang, D.; Qu, B.; Liu, P.; An, Z.; An, Z. Comprehensive evaluation and optimization of rural space heating modes in cold areas based on PMV-PPD. *Energy Build.* **2021**, *246*, 111120. [CrossRef]
53. Li, X.; Sheng, X.; Guo, Y.; Lu, X.; Wu, H.; Chen, Y.; Zhang, L.; Gu, J. Multifunctional HDPE/CNTs/PW composite phase change materials with excellent thermal and electrical conductivities. *J. Mater. Sci. Technol.* **2021**, *86*, 171–179. [CrossRef]
54. Savini, G.; Oréfice, R. Comparative study of HDPE composites reinforced with microtalc and nanotalcs: High performance filler for improving ductility at low concentration levels. *J. Mater. Res. Technol.* **2020**, *9*, 16387–16398. [CrossRef]
55. Chaudhry, A.; Lonkar, S.; Chaudhry, R.; Mabrouk, A.; Abdala, A. Thermal, electrical, and mechanical properties of highly filled HDPE/graphite nanoplatelets composites. *Mater. Today Proc.* **2020**, *29*, 704–708. [CrossRef]
56. Chavan, S.; Gumtapure, V.; Perumal, A. Numerical and experimental analysis on thermal energy storage of polyethylene/functionalized graphene composite phase change materials. *J. Energy Storage* **2020**, *27*, 101045. [CrossRef]
57. Staveckis, A.; Borodinecs, A. Impact of impinging jet ventilation on thermal comfort and indoor air quality in office buildings. *Energy Build.* **2021**, *235*, 110738. [CrossRef]